

PAPER • OPEN ACCESS

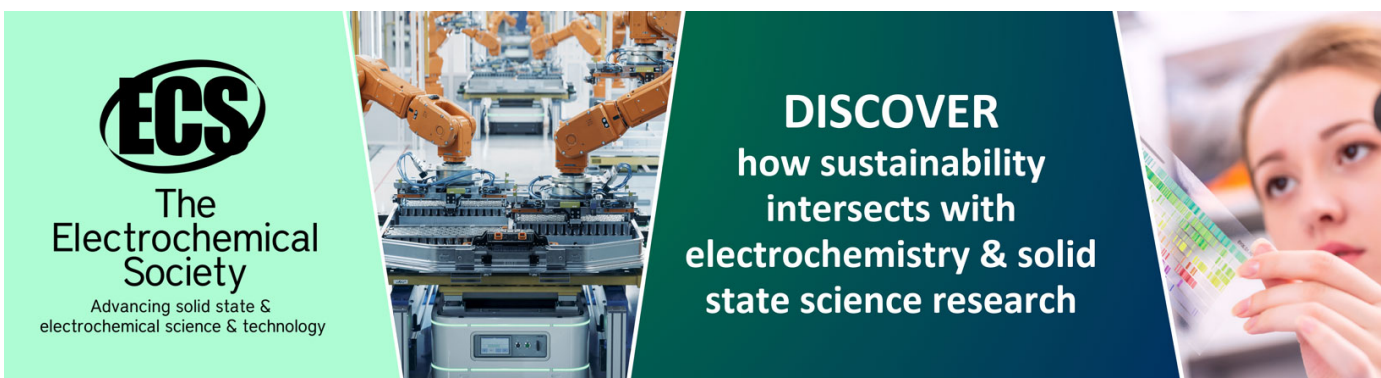
Dynamic properties analysis of ball screw feed system based on improved hybrid model

To cite this article: Xuan Sun *et al* 2022 *J. Phys.: Conf. Ser.* **2383** 012040

View the [article online](#) for updates and enhancements.

You may also like

- [An optimization method of acceleration and deceleration time of feed system based on load inertia](#)
Hao Zhou, Jianzhong Yang, Yongjie Guo et al.
- [A novel self-powered MR damper: theoretical and experimental analysis](#)
Guan Xinchun, Huang Yonghu, Ru Yi et al.
- [Remaining useful life prediction of ball screw based on integrating preload and precision](#)
Yishen Zhang, Changguang Zhou, Conghui Nie et al.



ECS
The
Electrochemical
Society
Advancing solid state &
electrochemical science & technology

DISCOVER
how sustainability
intersects with
electrochemistry & solid
state science research

Dynamic properties analysis of ball screw feed system based on improved hybrid model

Xuan Sun^{1*}, Xijun Liu², Minghao Liu¹

¹School of Mechanical Engineering, University of Jinan, Jinan 250022, China

²Huate Magnetolectric Technology Co., LTD, Weifang 262600, China

^{1*}me_sunx@ujn.edu.cn, ²1274559101@qq.com, ¹827181869@qq.com

Abstract—Ball screws are widely used as feed systems for machine tools due to their high transmission efficiency and long service life. However, the large inertia force generated by the ball screw in high-speed motion will excite its flexible mode and cause system vibration. In the actual working condition, the dynamics of the system will also change with the nut position and workpiece mass. In order to further study the modeling method and dynamic properties of the ball screw feed system, this paper firstly improves the traditional hybrid model by introducing an energy loss factor to modify the hysteresis damping of the model. Further, the rationality of the improved model is verified by hammer test. Finally, the model was used to analyze the dynamic properties of the system and to obtain the influence law of workpiece mass and nut position on the system natural frequency.

1. Introduction

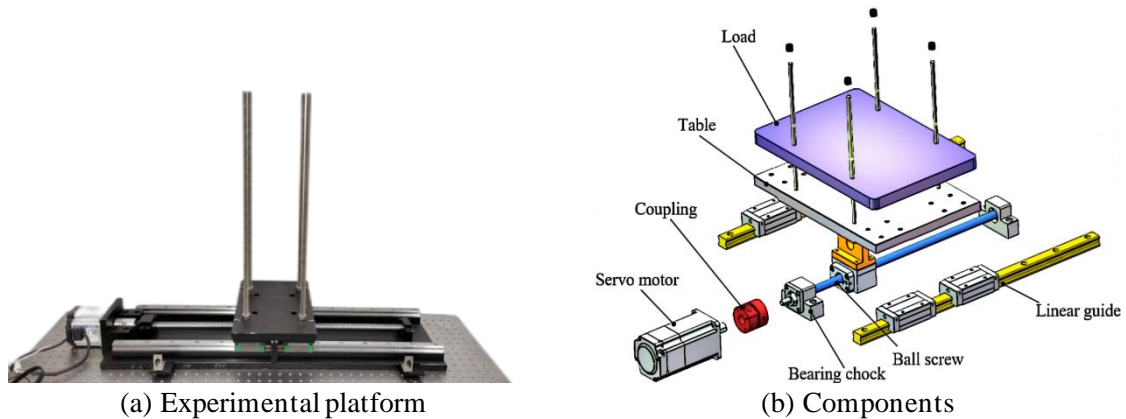
As the most common machine tool feed system, the motion control accuracy of ball screw directly determines the machining accuracy of machine tool [1]. At present, the main method of research on ball screw feed system control technology is to establish a control model and analyze the system dynamic properties according to the model, and then design a controller to meet the control requirements according to the dynamic properties of the system. At present, the commonly used modeling methods include finite element method [2], lumped mass method [3] and hybrid modeling method [4].

Considering that the ball screw will produce flexible modes at high speed, the hybrid model can describe the flexible vibration properties of the system more accurately than the finite element model and the lumped mass model. However, in actual working conditions, the dynamic properties of the system will also change with the change of nut position and workpiece mass. Therefore, it is necessary to improve the traditional hybrid model to improve the modeling accuracy, and further analyze the dynamic properties of the system to provide a theoretical basis for the design of the controller.

2. Rigid-flexible Coupling Hybrid Model of Ball Screw Feed System

Ball screw feed system is shown in Fig.1, and the system parameters are listed in table 1.





(a) Experimental platform

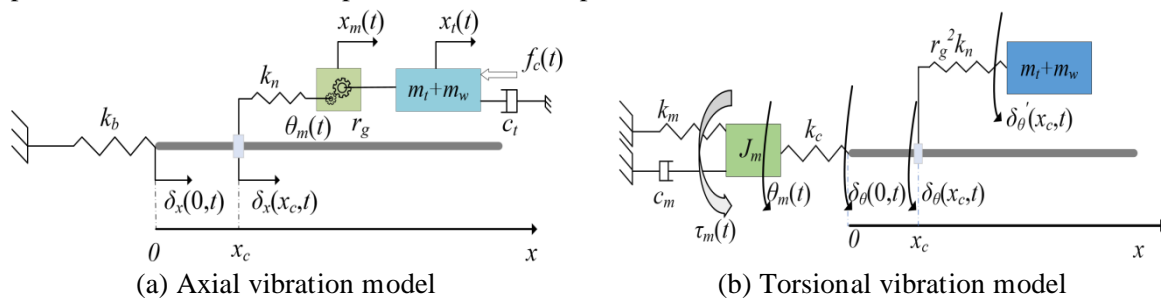
(b) Components

Fig.1 Ball screw feed system

Table 1. Parameters of ball screw feed system

Parameter name	Symbol	Value	Unit
Lead of screw	P_t	20	mm
Transmission ratio of screw	r_g	3.1831×10^{-3}	m/rad
Length of screw	l_s	746.5	mm
Density of screw	ρ_s	7830	kg/m ³
Diameter of screw	d_s	20	mm
Young 's modulus of screw	E_s	2.2×10^{11}	Pa
Shear modulus of screw	G_s	0.8×10^{11}	Pa
Worktable mass	m_t	10	kg
Torsional stiffness of coupling	k_c	2.681×10^4	N/m
Rotary inertia of screw	J_s	0.4689×10^{-5}	kg·m ²
Rotational inertia of motor shaft	J_m	1.56×10^{-4}	kg·m ²
Rotational inertia of coupling	J_c	3.66×10^{-5}	kg·m ²
Equivalent viscous damping of motor shaft	c_m	0.026	Nm/rad/s
Equivalent viscous damping of table	c_t	0	Nm/rad/s
Axial stiffness of bearing	k_b	6.21×10^7	N/m
Torsional stiffness of screw nut joint	k_n	1.37×10^8	N/m

As shown in Fig.2, based on the hybrid modeling method proposed by Varanasi and Nayfeh [5], the rigid-flexible coupling dynamic equation is developed and the system dynamic equation is expressed as a function of nut position x_c and workpiece mass m_w .



(a) Axial vibration model

(b) Torsional vibration model

Fig.2 Rigid-flexible coupling hybrid model

In the axial vibration model, k_b , δ_x , k_n , r_g , θ_m , x_c , x_m , x_t , m_t , m_w , f_c and c_t represent the axial stiffness of the bearing, the axial deformation of the screw, the axial stiffness of the screw nut joint, the transmission ratio of the screw, the rotation angle of the motor shaft, the nut position, the equivalent linear displacement of the motor shaft, the linear displacement of the table, the mass of the table, the

workpiece mass, the external force of the table and the equivalent viscous damping of the table, respectively.

In the torsional vibration model, k_m , c_m , τ_m , J_m , k_c , $\delta\theta$, $\delta\theta'$, and $r_g^2 k_n$ represent the torsional stiffness of the motor shaft, the equivalent viscous damping of the motor shaft, the output torque of the motor, the rotational inertia of the motor shaft, the torsional stiffness of the coupling, the torsional deformation of the screw, the torsional deformation of the table and the torsional flexibility of the screw nut joint, respectively.

The rigid-flexible coupling hybrid model is written as matrix expression:

$$M \begin{pmatrix} \ddot{x}_m(t) \\ \ddot{x}_t(t) \end{pmatrix} + C \begin{pmatrix} \dot{x}_m(t) \\ \dot{x}_t(t) \end{pmatrix} + K \begin{pmatrix} x_m(t) \\ x_t(t) \end{pmatrix} = \begin{pmatrix} f_m(t) \\ f_c(t) \end{pmatrix} \quad (1)$$

where, $f_m = \tau_m / r_g$ represents the equivalent force of the torque applied by the motor, M , C and K represent the total mass matrix, damping matrix and stiffness matrix of the system respectively, which are expressed as:

$$M = \begin{bmatrix} m_{11}(x_c) & m_{12}(x_c) \\ m_{21}(x_c) & m_{22}(x_c, m_w) \end{bmatrix} = \begin{bmatrix} (J_m + J_c + J_{11}) / r_g^2 + m_s & J_{12} / r_g^2 - m_s \\ J_{12} / r_g^2 - m_s & J_{21} / r_g^2 + m_s + m_t + m_w \end{bmatrix} \quad (2)$$

$$C = \begin{bmatrix} c_m / r_g^2 & 0 \\ 0 & c_t \end{bmatrix} \quad (3)$$

$$K = k \begin{bmatrix} 1 & -1 \\ -1 & 1 \end{bmatrix} \quad (4)$$

where, J_{11} , J_{12} , J_{21} and J_{22} represent the moment of inertia of the screw contribution to different degrees of freedom, m_s represents the equivalent mass of the screw, k represents the total equivalent stiffness of the system. The specific expression of each parameter is:

$$k(x_c) = \left[\frac{1}{k_b} + \frac{x_c}{E_s A_s} + \frac{2}{k_n} + r_g^2 \left(\frac{1}{k_c} + \frac{x_c}{G_s J_s} \right) \right]^{-1} \quad (5)$$

$$m_s(x_c) = \frac{\rho_s A_s x_c}{3} \left[\left(\frac{k}{k_1} \right)^2 + \frac{k^2}{k_1 k_b} + \left(\frac{k}{k_b} \right)^2 \right] + \rho_s A_s (l_s - x_c) \left(\frac{k}{k_1} \right)^2 \quad (6)$$

$$k_1(x_c) = \left(\frac{x_c}{E_s A_s} + \frac{1}{k_b} \right)^{-1} \quad (7)$$

$$J_{11}(x_c) = \rho_s J_s l_s \left(1 - r_g^2 \frac{k}{k_2} \right)^2 \quad (8)$$

$$\left\{ \frac{x_c}{3l_s} \left[1 + \left(1 - r_g^2 \frac{k}{k_c} \right) \left(1 - r_g^2 \frac{k}{k_2} \right)^{-1} + \left(1 - r_g^2 \frac{k}{k_c} \right)^2 \left(1 - r_g^2 \frac{k}{k_2} \right)^{-2} \right] + \left(1 - \frac{x_c}{l_s} \right) \right\}$$

$$k_2(x_c) = \left(\frac{x_c}{G_s J_s} + \frac{1}{k_c} \right)^{-1} \quad (9)$$

$$J_{12}(x_c) = J_{21}(x_c) = \rho_s J_s l_s r_g^2 \frac{k}{k_2} \left\{ \frac{x_c}{l_s} \left[\frac{1}{6} + \frac{k_2}{k_c} \left(\frac{1}{2} - r_g^2 \frac{k}{3k_c} \right) - \frac{2x_c}{3l_s} \right] + \left(1 - \frac{2x_c}{3l_s} \right) \left(1 - r_g^2 \frac{k}{k_c} \right) \right\} \quad (10)$$

$$J_{22}(x_c) = \rho_s J_s l_s \left(r_g^2 \frac{k}{k_2} \right)^2 \left[\frac{x_c}{3l_s} \left(1 + \frac{k_2}{k_c} + \frac{k_2^2}{k_c^2} \right) + \left(1 - \frac{x_c}{l_s} \right) \right] \quad (11)$$

The parameters in equation (5) to equation (11) are given in table 1. And the Laplace change of equation (1) can be obtained as follows:

$$(Ms^2 + Cs + K) \begin{pmatrix} x_m(t) \\ x_t(t) \end{pmatrix} = \begin{pmatrix} f_m(t) \\ f_c(t) \end{pmatrix} \quad (12)$$

So the transfer function of rigid-flexible coupling hybrid model is:

$$G(s) = \begin{bmatrix} G_{11} & G_{12} \\ G_{21} & G_{22} \end{bmatrix} = (Ms^2 + Cs + K)^{-1} \tag{13}$$

3. Modification of Model Hysteresis Damping by Introducing Energy Loss Factor

For the established rigid-flexible coupling hybrid model, set $x_c=300[\text{mm}]$, $m_w=0[\text{kg}]$, draw the frequency response curve as shown in Fig.3.

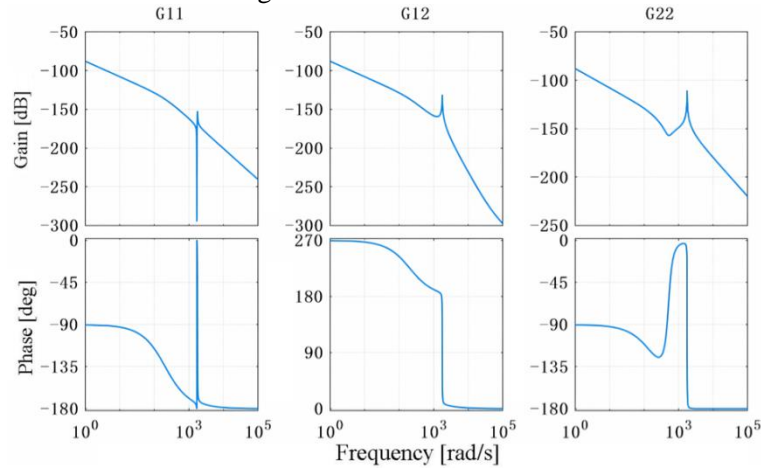


Fig.3 Frequency response curve of rigid-flexible coupling hybrid model

It can be seen from Fig.3 that the vibration amplitude of the system has a significant mutation at the resonant frequency, and the change of G_{11} is the most obvious. Using MATLAB to solve the eigenvalues and eigenvectors of G_{11} , the resonant frequency is 1726.8 rad/s, and the damping ratio is 0.52%. Considering the amplitude mutation caused by the small damping ratio, the energy loss factor is introduced to modify the hysteresis damping of the model.

Fig.4 shows the introduction diagram of energy loss factor, and the complex stiffness $k_x(1+j\eta)$ is used to replace the original stiffness of each concentrated spring in the model. k_x , η and j represent the original stiffness, energy loss factor and imaginary number unit, respectively.

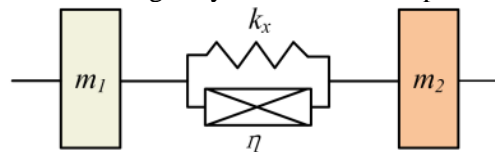


Fig.4 The introduction diagram of energy loss factor

The total equivalent stiffness of the system after using the complex stiffness is expressed as:

$$\hat{k}(x_c)(1+j\eta_e) = \left[\frac{1}{k_b(1+j\eta)} + \frac{x_c}{E_s A_s} + \frac{2}{k_n(1+j\eta)} + r_g^2 \left(\frac{1}{k_c(1+j\eta)} + \frac{x_c}{G_s J_s} \right) \right]^{-1} \tag{14}$$

The energy loss factor η of the spring is set to 0.053. The frequency response curve of the modified hysteresis damping is drawn and compared with that before the modification, as shown in Fig.5.

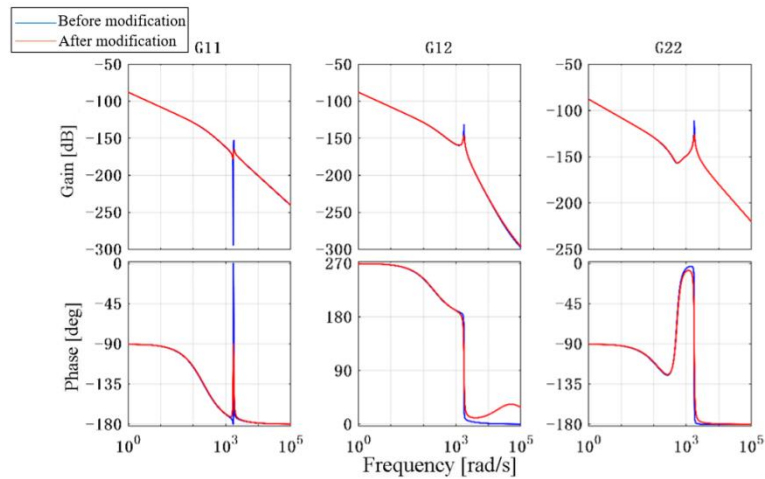


Fig.5 Comparison of frequency response curves before and after modification

It can be seen from Fig.5 that the amplitude mutation after modification is significantly reduced. The modified resonant frequency is 1782.4 rad/s and the damping ratio is 2.87% by solving the eigenvalues and eigenvectors of G_{11} . Since the damping ratio is between 1% and 3%, the improved rigid-flexible coupling hybrid model is more reasonable than before.

The frequency response curve including the first three orders natural frequencies of the system obtained by hammer test is shown in Fig.6. The test value of the first three orders natural frequencies of the system are 266.72Hz, 310.82Hz and 485.26Hz, respectively. The theoretical calculation values of the first three orders natural frequencies of the system obtained by the improved model are 283.68Hz, 332.55Hz and 478.43Hz, respectively. The theoretical deviation are 6.36%, 6.70% and 1.41%, respectively. So the accuracy of the improved model is proved.

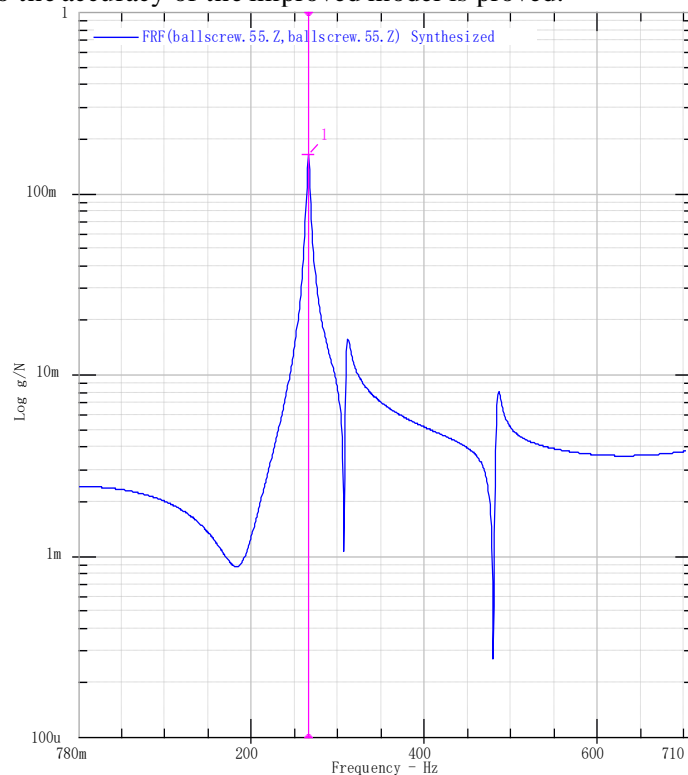


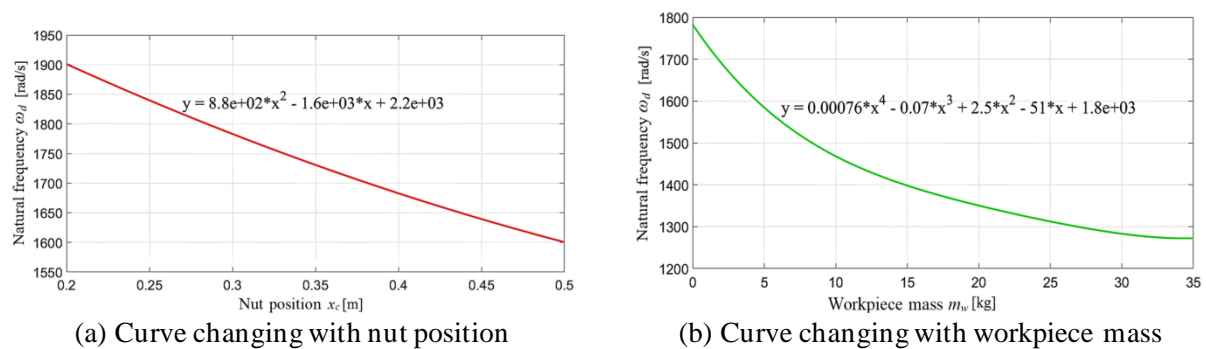
Fig.6 Frequency response curve of hammer test

4. Analysis on the Influence Law of Parameter Variation on System properties

Based on the built-up hybrid model, the influence law of nut position and workpiece mass on the system dynamic properties is researched with the natural frequency as the system properties indicators.

Firstly, the workpiece mass $m_w=0$ [kg] is set, and then the nut position x_c is changed to solve the natural frequency of the system. The change curve of the natural frequency with the nut position is fitted. It can be seen from Fig.7(a) that with the increase of nut position, the natural frequency of the system decreases and shows a quadratic polynomial downward trend.

Secondly, the nut position $x_c=0.3$ [m] is set, and then the workpiece mass m_w is changed to solve the natural frequency of the system. The change curve of the natural frequency with the workpiece mass is fitted. It can be seen from Fig.7(b) that with the increase of workpiece mass, the natural frequency of the system decreases and shows a downward trend of quartic polynomial.



(a) Curve changing with nut position

(b) Curve changing with workpiece mass

Fig.7 Curve of natural frequency changing with nut position and workpiece mass

5. Conclusion

In this paper, an improved hybrid model of ball screw feed system is established and the dynamic properties of the system are analyzed. Firstly, the hysteresis damping in the traditional hybrid model is modified by introducing the energy loss factor. Secondly, the hammer test verifies that the model has high precision. Finally, the influence of nut position and workpiece mass on the system natural frequency is researched based on the improved hybrid model. The research content of this paper provides a theoretical basis for the design of high-precision controller of ball screw feed system.

Acknowledgments

This study was supported by Key Research & Development Program of Shandong Province (No. 2019GGX104101), and Postgraduate Joint Training Base Project.

References

- [1] Liu T, Li C, Zhang Y, et al. (2021) Active Coolant Control Onto Thermal Behaviors of Precision Ball Screw Unit[J]. The International Journal of Advanced Manufacturing Technology, 119(3-4): 1867-1882.
- [2] Wang H, Li F, Cai Y, et al. (2020) Experimental and theoretical analysis of ball screw under thermal effect[J]. Tribology International, 152(2): 106-143.
- [3] Yu H, Feng X. (2016) Dynamic Modeling and Spectrum Analysis of Macro-Macro Dual Driven System[J]. Journal of Computational and Nonlinear Dynamics, 11(4): 208-213.
- [4] Zhang H, Hui L, Chao D, et al. (2018) Dynamics analysis of a slender ball-screw feed system considering the changes of the worktable position[J]. Archive Proceedings of the Institution of Mechanical Engineers Part C Journal of Mechanical Engineering Science, 233(2): 95-106.
- [5] VARANASI K K, NAYFEH S A. (2004) The Dynamics of Lead-Screw Drives: Low-Order Modeling and Experiments[J]. Journal of Dynamic Systems, Measurement, and Control, 126(2): 388-396.